energies

MDPI

Article

BFC-POD-ROM Aided Fast Thermal Scheme Determination for China's Secondary Dong-Lin Crude Pipeline with Oils Batching Transportation

Dongxu Han [1], Qing Yuan [2], Bo Yu [1,*], Danfu Cao [3] and Gaoping Zhang [3]

[1] School of Mechanical Engineering, Beijing Key Laboratory of Pipeline Critical Technology and Equipment for Deepwater Oil & Gas Development, Beijing Institute of Petrochemical Technology, Beijing 102617, China; handongxubox@bipt.edu.cn

[2] National Engineering Laboratory for Pipeline Safety, Beijing Key Laboratory of Urban Oil and Gas Distribution Technology, China University of Petroleum, Beijing 102249, China; 2015314026@student.cup.edu.cn

[3] Storage and Transportation Company, Sinopec Group, Xuzhou 221000, China; caodf.gdcy@sinopec.com (D.C.); zhanggp.gdcy@sinopec.com (G.Z.)

* Correspondence: yubobox@bipt.edu.cn; Tel.: +86-10-8129-2805

Received: 14 August 2018; Accepted: 3 October 2018; Published: 7 October 2018

Abstract: Since the transportation task of China's Secondary Dong-Lin crude pipeline has been changed from Shengli oil to both Shengli and Oman oils, its transportation scheme had to be changed to "batch transportation". To determine the details of batch transportation, large amounts of simulations should be performed, but massive simulation times could be costly (they can take hundreds of days with 10 computers) using the finite volume method (FVM). To reduce the intolerable time consumption, the present paper adopts a "body-fitted coordinate-based proper orthogonal decomposition reduced-order model" (BFC-POD-ROM) to obtain faster simulations. Compared with the FVM, the adopted method reduces the time cost of thermal simulations to 2.2 days from 264 days. Subsequently, the details of batch transportation are determined based on these simulations. The Dong-Lin crude oil pipeline has been safely operating for more than two years using the determined scheme. It is found that the field data are well predicted by the POD reduced-order model with an acceptable error in crude oil engineering.

Keywords: fast thermal simulation; crude oil pipeline; batch transportation; body-fitted coordinate-based proper orthogonal decomposition reduced-order model (BFC-POD-ROM); transport scheme determination

1. Introduction

This paper focuses on the fast thermal scheme determination for oils batching transportation in China's Secondary Dong-Lin crude pipeline, which is obtained by the proper orthogonal decomposition based reduced-order model (POD-ROM) method. Thus, in this section, the Secondary Dong-Lin crude oil pipeline and the thermal simulations for batch transportation are briefly reviewed first. The POD reduced-order model and applications on the crude pipeline's thermal simulation are reviewed subsequently.

The Secondary Dong-Lin pipeline (also called Dongying-Linyi parallel pipeline), owned by the Sinopec Company, is an important crude oil transportation pipeline across the Shandong province in China. The pipeline is designed to transport the Shengli (SL) crude oil to Linyi, which is produced in the Shengli oilfields in Dongying. Since the fluidity of SL oil is poor, the heated transportation process was adopted before October 2015 [1].

The imported Oman oil (OM), however, with a low condensation point (0 °C) and good fluidity, was planned to be transported in the Secondary Dong-Lin pipeline by October 2015. Thus, its task turned to the transportation of both the imported OM oil and produced SL oil, which totally deviated from the original design. The "batch transportation with different oil temperatures" must be adopted and tremendous corresponding thermal simulations were required.

Different from the batch transportation of petroleum products [2], the thermal characteristics of crude oils' batch transportation are very complex because the different crude oils must be transported in different temperatures due to their large fluidity differences. Batch pipelining with different oil temperatures was first applied to the Pacific Pipeline System, situated in California USA. and commissioned in 1999 [3,4]. Unfortunately, few technique reports are available for its thermal characteristics. Recently, some studies have been performed to discover the thermal behaviors of batch pipelining of crude oils. Cui et al. [5] studied the thermal periodic characteristics for crude oils' batch transportation. Wang et al. [6] gave a report on the thermal and hydraulic behaviors. Yuan [7] studied the thermal characteristics of crude oil batch pipelining with inconstant flow rates.

All the thermal simulations in the above references, however, use the finite volume method (FVM), which is not very suitable for thermal scheme determinations of real engineering pipelines, such as the Secondary Dong-Lin pipeline in the present paper. Moreover, to obtain a proper operational scheme, thousands of thermal simulations should be done using FVM, consuming hundreds of days of simulation even with 10 computers' parallel computing. Thus, to overcome this problem, this paper adopts the POD reduced-order model to significantly improve the simulation speed.

To describe a physical problem with a reduced-order model, the first step is to obtain a series of basis functions, which can express accurately the problem with a small degree of freedom. Normally, the basis function is extracted from a large amount of data by mathematical methods, such as POD [8,9], empirical mode decomposition (EMD) [10], or dynamic mode decomposition (DMD) [11]. POD is adopted in this paper for model reduction. The reduced-order model (ROM), based on POD, can not only describe the problems, but also accelerate the calculations. Thus, this technique is studied extensively for heat transfer and is widely used in engineering.

Regarding the field of heat transfer, Banerjee et al. [12] established a POD-Galerkin ROM for heat transfer based on a finite element method, and Raghupathy et al. [13] established a boundary condition-independent ROM by combining a POD-Galerkin method with a finite volume method. The research of POD-Galerkin ROM are becoming increasingly mature, thus, it is widely applied to engineering [14–18].

The POD reduced-order models above, however, cannot be applied to the thermal simulation of the Secondary Dong-Lin pipeline. To the author's knowledge, the POD-based ROMs in the relevant literature are established for a fixed physical domain, although the boundary conditions and initial fields might vary, while, for the Secondary Dong-Lin crude oil pipeline, the physical domains vary along the pipeline since its diameter and buried depth is different from place to place. To solve this problem, the current research group first proposes a "body-fitted coordinate-based proper orthogonal decomposition reduced-order model" (BFC-POD-ROM) for the heat transfer problem [19,20], in which physical domains with different shapes or sizes can be mapped to the same computational domain.

Therefore, in this paper, BFC-POD-ROM is adopted to obtain the fast thermal simulation of China's Secondary Dong-Lin crude pipeline. Then, the detailed thermal scheme is determined based on the simulations. Finally, the predicted oil temperature distributions are verified through the field data of the Secondary Dong-Lin crude pipeline.

2. Oil Transportation Scheme and Thermal State of Secondary Dong-Lin Pipeline

2.1. Basic Situation

The Secondary Dong-Lin pipeline (constructed in 1999) was originally designed as a supplementary crude pipeline for the Old Dong-Lin pipeline (constructed in 1979), since the old one could not accomplish the crude transportation task by itself.

Prior to October 2015, the main task of the Secondary Dong-Lin pipeline was to transport the SL oil from the Sheng-Li oilfield in Dongying to the consumers in Linyi. Additionally, it transported the SL oil produced in the Bin-Nan oil production factory (also called Bin-Nan oil) through injection (See Figure 1), while the old one was arranged to transport the imported OM oil.

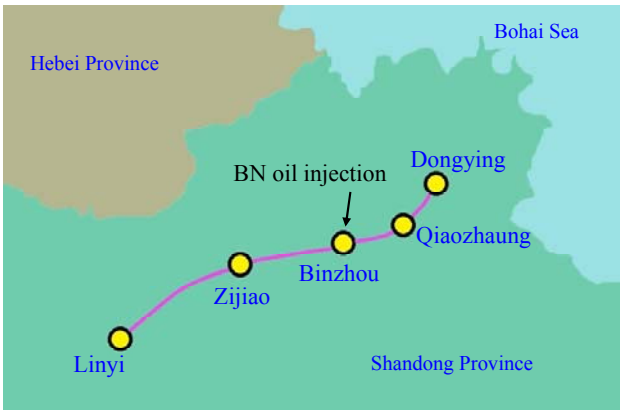

Figure 1. Route of the Secondary Dong-Lin crude pipeline.

The whole secondary pipeline is located in the Shandong Province of China. The route of the Secondary Dong-Lin pipeline is drawn in the map (See Figure 1) and its sketch map with details is found in Figure 2.

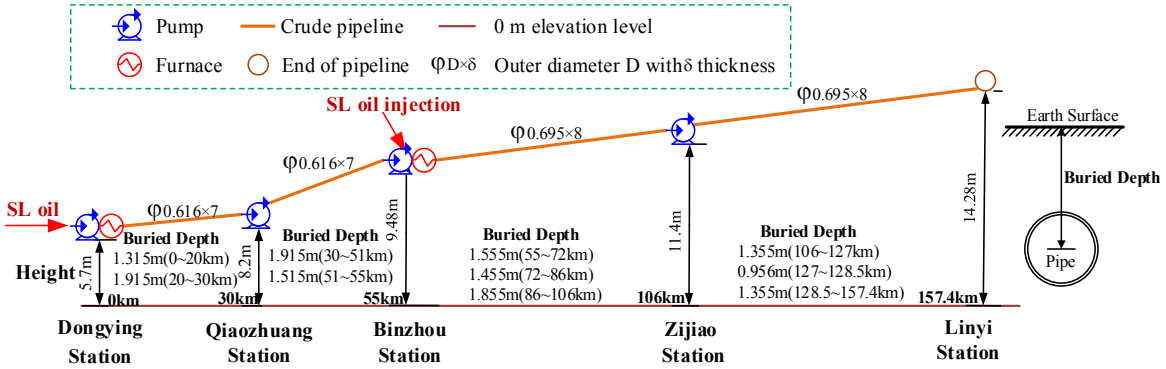

Figure 2. Sketch map of the Secondary Dong-Lin crude pipeline.

Figure 2 shows the total length of the pipeline is 157.4 km with a slight elevation change. Four pump stations (Dongying, Qiaozhuang, Binzhou, and Zijiao stations) are separately located in the positions of 0 km, 30 km, 55 km, and 106 km along the pipeline. Among them, the Dongying Station and Binzhou Station are equipped with furnaces, which means the crude oil can be heated in these two stations. The outer diameter of the pipeline is 0.616 m with a wall thickness of 7 mm before Binzhou station and becoming 0.695 m and 8 mm after Binzhou Station. The buried depth of the pipeline varies along the pipeline, with the minimum depth at 0.956 m and the maximum at 1.915 m.

Since the old Dong-Lin pipeline is too old and should be decommissioned as per regulations, the Secondary Dong-Lin pipeline was planned, by Sinopec Company, to take over the transportation tasks

of the Old Dong-Lin pipeline after November 2015. Thus, the SL and OM oils would be transported in the same pipeline.

As demanded by the downstream consumer, the imported OM oil is of much better chemical quality and should not be mixed with SL oil. Therefore, the batching transportation is the only choice for the Sinopec Company (See Figure 3). Additionally, to decrease the viscosity of SL oil, the company decided to blend some OM oil into the SL oil at the beginning of the pipeline. The blended oil is named SL_{OM} oil in this paper. The optimal amount of SL_{OM} compositions also needs to be determined by thermal simulation. The rough scheme of batch transportation is shown in Figure 3.

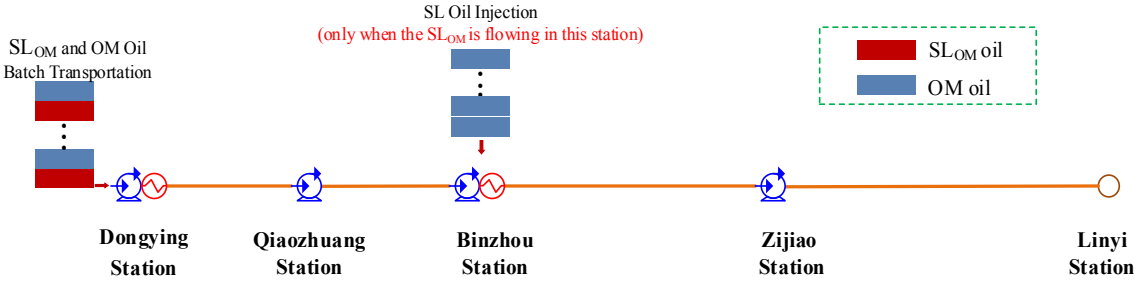

Figure 3. Sketch map of the batch transportation scheme.

Figure 3 shows the SL_{OM} oil and the OM oil are pumped alternately into the pipeline from the Dongying station, which is the first station and the beginning of the pipeline. To avoid degrading the quality of OM oil, the SL oil can only be injected when the oil flowing in Binzhou station is SL_{OM} oil.

Even though the rough scheme is easy to be pictured, to determine the safe and economic detailed transport scheme, many thermal analyses should be performed. The thermal state before and with batch transportation are introduced as follows.

2.2. Thermal State of the Dong-Lin oil Pipeline

2.2.1. Thermal State before the Batch Transportation

Prior to the batch transportation, the crude oils in the Secondary Dong-Lin oil pipeline were SL oil. Since the condensation point of SL is 11 °C, as shown in Table 1, it might be gelled in the pipeline in the winter when the environmental temperature is lower than the condensation point [21]. This could lead to scrapping the pipeline, which is unacceptable for the Sinopec Company.

Table 1. Basic physical properties of Shengli (SL) and Oman (OM) oil.

Oil	ρ_o (kg/m^3)	$c_{p,o}$ (J/kg·°C)	θ_{cp} (°C)	μ (Pa·s)
SL oil	937	2000	11	Polynomial $P_n(T)$
OM oil	868	2100	0	See Figure 4
SL_{OM} oil	Can be predicted through properties of SL oil and OM oil by equations in Ref. [22]. Sinopec also did extensive testing on the SL_{OM} oil with different ratios of SL and OM oil.			

Thus, before October 2015, the heating process was adopted in the Secondary Dong-Lin pipeline to ensure the safety of the pipeline. Additionally, the heat process can also lower the viscosity and improve the fluidity of SL oil, which can reduce the power cost at pumps. Since the temperature of oil flowing out of Dongying Station and Binzhou station was kept at a certain value, the thermal state was approximately steady. Figure 5 gives the oil temperature distribution along the pipeline in October 2015.

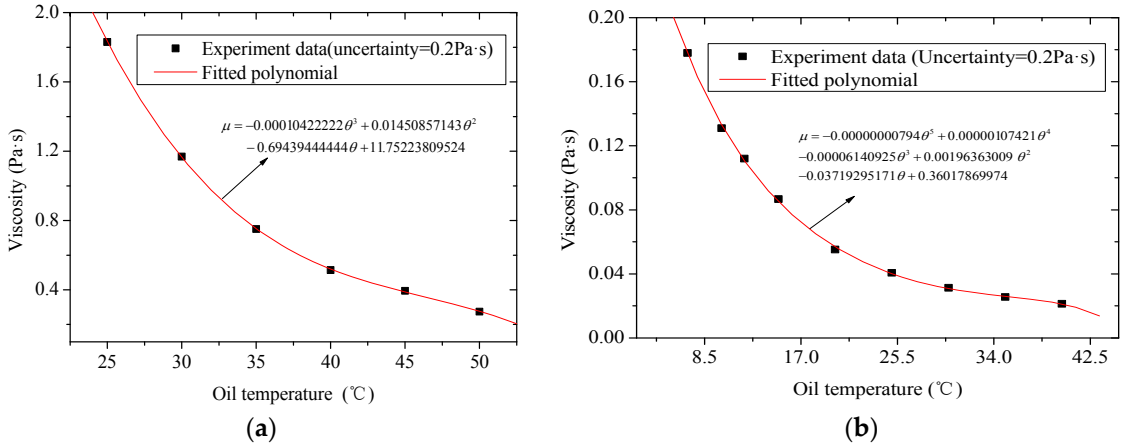

Figure 4. Viscosity-temperature curves and fitted equations of: (**a**) Shengli (SL) oil; and (**b**) Oman (OM) oil.

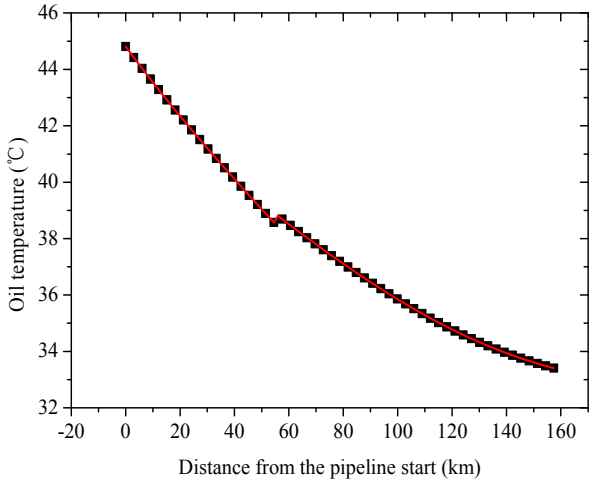

Figure 5. Oil temperature distribution along the pipeline in October 2015.

2.2.2. Thermal State of the Batch Transportation

Table 1 and Figure 4 show the fluidity differences of the SL_{OM} and OM oils are very significant at the same temperature. To save the energy consumed by furnaces, the SL_{OM} and OM oil are transported at different temperatures (See Figure 6). The SL_{OM} oil with high temperature is also called "hot oil" while the OM oil is called "cool oil". Figure 6 gives the typical oil temperature distribution flowing out of the Dongying station during a certain time frame.

Since the oil temperature varies, the thermal state of the whole pipeline is unsteady and changes dramatically when the SL_{OM} oil and OM oil alternate. Additionally, the thermal behaviors are so complicated that the thermal analysis to determine the detailed transportation scheme must be done by numerical simulations. Considering the changing environmental temperature from month to month, to clarify the thermal behavior of a certain case, the current authors must simulate the pipeline's thermal behavior from the beginning to the coldest month. This can be very time consuming.

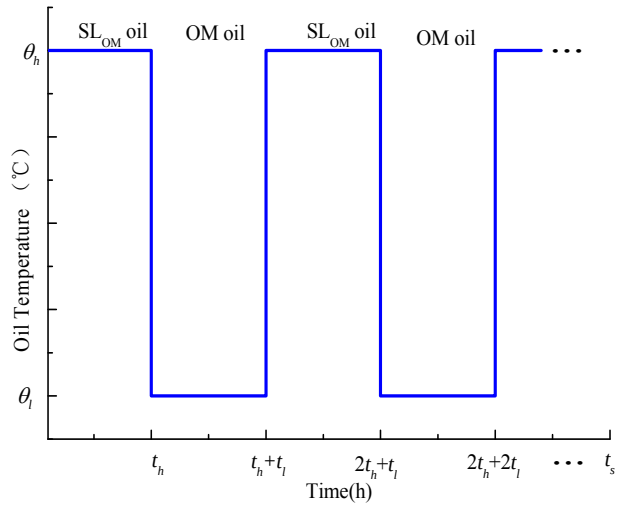

Figure 6. Oil temperature flowing out of Dongying station versus time in a certain time frame.

2.3. Detailed Batch Transportation Scheme to be Determined

The thermal-related operating parameters in batch transportation are as follows: The compositions of SL_{OM} (critical to its fluidity), flow fluxes of SL_{OM} and OM oils, transportation time of each patch (value of t_h and t_l in Figure 6), temperatures of SL_{OM} and OM oil flowing out of the Dongying station (value of θ_h and θ_l in Figure 6), how much and when the oil should be heated by the furnaces in Binzhou station, and the temperature and flux of SL oil injected in Binzhou station.

Thus, thousands of cases should be simulated to find a safe, economical, and relatively optimal transportation scheme. The time consumption of simulations by the frequently-used FVM can be hundreds of days on a personal computer, which is unacceptable for engineering practices. To quickly determine the thermal scheme for this paper, the current authors applied the body-fitted coordinate-based POD reduced-order model developed by their research group to the pipeline thermal simulation. The method is elaborately introduced in Section 4.

3. Physical and Mathematical Model for Secondary Dong-Lin Pipeline

Regarding the batch transportation of the Secondary Dong-Lin pipeline, as shown in Figure 3, sometimes the oil temperature can be higher than that of the surrounding pipe wall and soil, while the opposite is true at other times. This leads to the complicated, unsteady thermal state of the pipeline. Since the pipeline is 154.7 km long, the full 3-D simulation is impractical for the unsteady heat transfer in the pipeline. Thus, the problem is simplified by splitting the pipeline into a series of thermal elements, as shown in Figure 7.

Figure 7 shows the thermal element consists of a pipeline cross-section and a segment of the axial pipeline. The physical and mathematical model of the pipeline cross-section and the axial pipeline (namely the oil stream) are introduced in Sections 3.1 and 3.2, respectively.

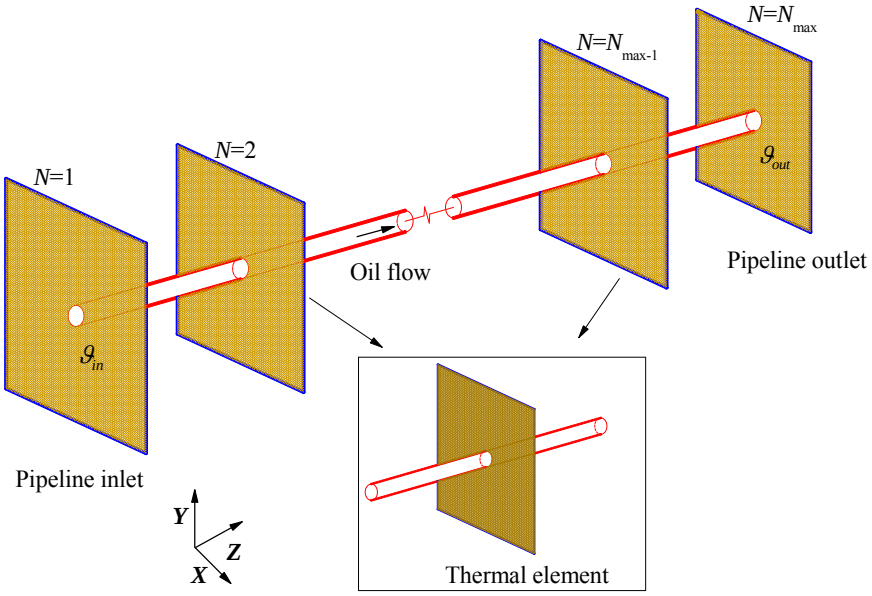

Figure 7. The simplification of the whole 3-D pipeline.

3.1. Physical and Mathematical Model of the Pipeline Cross-section

The sketch map of the pipeline cross-section is shown in Figure 8a. Since an oil pipe is buried in a certain place, it will influence the local temperature field in the soil. The further the soil from the pipe the smaller the influence can be, so it can be neglected for soil very far from the pipe. Thus, to simplify the simulation, it is believed there is a "thermal influence region" (See Figure 8a) of the oil pipe. It is assumed the oil pipe has no impact on the soil temperature field outside the influence region. According to the literature [6] and engineering experience, the thermal influence region of the hot crude oil pipeline is within 10 m, which means L = 10 m and H = 10 m, as shown in Figure 8a.

Considering the symmetry of the pipeline section (See Figure 8a), the physical model is obtained and is shown in Figure 8b. The physical domain is governed by heat conduction and the whole boundary can be divided into six parts, which are Lines O-A, A-B, B-C, C-D'-D, F-F'-O and semicircle D-E-F (See Figure 8b).

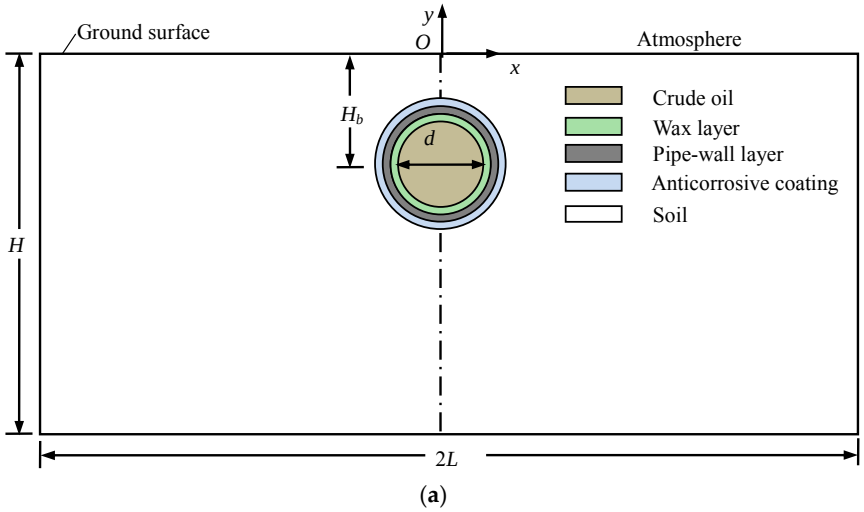

(**a**)

Figure 8. *Cont.*

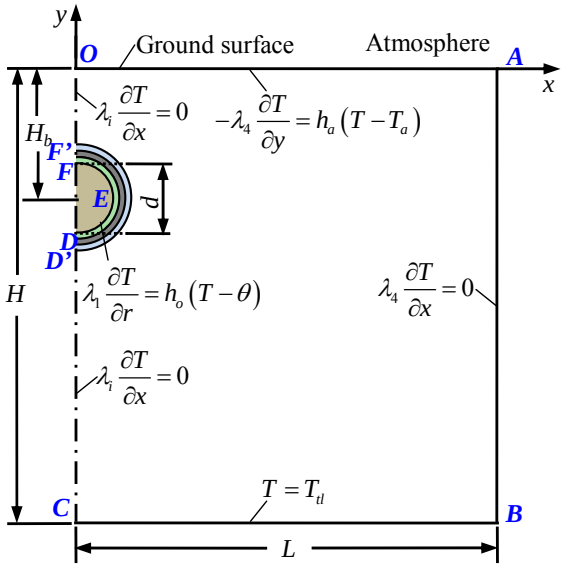

(**b**)

Figure 8. Thermal influence region and physical model of the pipeline cross-section on Cartesian coordinates: (**a**) Thermal influence region; (**b**) physical model.

Considering line O-A and semicircle D-E-F, they are convective heat transfer boundaries that describe the heat convection between the thermal region and the outside (air and oil, respectively, for Line O-A and semicircle D-E-M). Regarding Line A-B, it is the thermal adiabatic boundary, which means the oil pipe has no influence on the soil outside the thermal region. Looking at Line B-C, the temperature has a fixed value, which is the temperature of the thermostat soil layer. Considering Line C-D'-D and Line F-F'-O, they are symmetric boundary conditions.

Using Cartesian coordinates, the governing equation is shown in Equation (1):

$$\frac{\partial(\rho_i c_{p,i} T)}{\partial t} = \frac{\partial}{\partial x}(\lambda_i \frac{\partial T}{\partial x}) + \frac{\partial}{\partial y}(\lambda_i \frac{\partial T}{\partial y}) \tag{1}$$

where T stands for the temperature field in the cross-section. The subscript, i = 1, 2, 3, 4, stands for the wax layer [23], pipe-wall layer, anticorrosive layer (also called "the three layers"), and soil region around the pipe, respectively.

To take advantage of the BFC-based POD reduced-order model stated in the "Introduction", all the simulations in this paper are on body-fitted coordinates. To obtain the mathematical model on body-fitted coordinates, the physical domain is mapped to the calculation domain (See Figure 9) on body-fitted coordinates.

Correspondingly, Equation (1) is mapped to body-fitted coordinates and the governing equation for BFC is obtained as Equation (2) [24]:

$$J\frac{\partial(\rho_i c_{p,i} T)}{\partial t} = \frac{\partial}{\partial \xi}\left[\frac{\lambda_i}{J}\left(\alpha\frac{\partial T}{\partial \xi} - \beta\frac{\partial T}{\partial \eta}\right)\right] + \frac{\partial}{\partial \eta}\left[\frac{\lambda_i}{J}\left(\gamma\frac{\partial T}{\partial \eta} - \beta\frac{\partial T}{\partial \xi}\right)\right] \tag{2}$$

where, $\alpha = x_\eta^2 + y_\eta^2, \beta = x_\xi x_\eta + y_\xi y_\eta, \gamma = x_\xi^2 + y_\xi^2, J = x_\xi y_\eta - x_\eta y_\xi$.

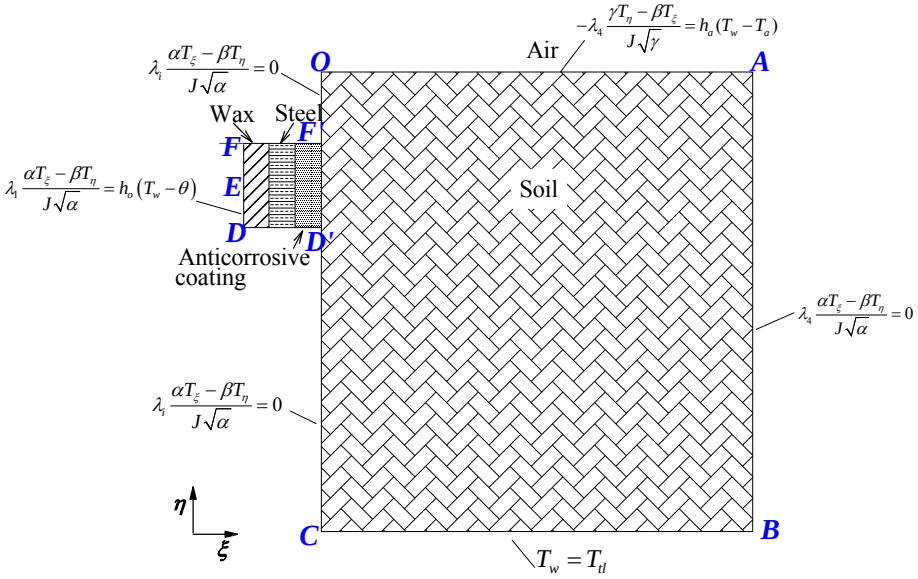

Figure 9. Physical model of pipeline cross-section on body-fitted coordinate.

Similarly, the boundary conditions on BFC also are obtained by mapping the boundary conditions on Cartesian coordinates, as shown in Figure 8b. The gained boundary conditions are as follows (See Figure 9):

$$\text{The boundary O-A}: \quad -\lambda_4\frac{\gamma T_\eta-\beta T_\xi}{J\sqrt{\gamma}}=h_a(T_w-T_a) \tag{3}$$

$$\text{The boundary A-B}: \quad -\lambda_4\frac{\alpha T_\xi-\beta T_\eta}{J\sqrt{\alpha}}=0 \tag{4}$$

$$\text{The boundary B-C}: \quad T_w=T_{tl} \tag{5}$$

$$\text{The boundary C-D}'\text{-D and F-F}'\text{-O}: \quad \lambda_i\frac{\alpha T_\xi-\beta T_\eta}{J\sqrt{\alpha}}=0 i=1,2,3,4 \tag{6}$$

$$\text{The boundary D-E-F}: \quad \lambda_1\frac{\alpha T_\xi-\beta T_\eta}{J\sqrt{\alpha}}=h_o(T_w-\theta) \tag{7}$$

Used in Equations (3)–(7), the subscript, w, stands for the wall in contact with the oil stream; subscripts, o and a, stand for oil and air, respectively; and the subscript, tl, stands for the thermostat layer.

Normally, the governing equation, Equation (2), is solved by FVM under the boundary conditions using Equations (3)–(7). Compared with the reduced order method introduced in Section 4, this currently presented method is called the "full order method".

3.2. Physical and mathematical model of the oil stream

The pipeline thermal simulation is the coupling of the cross-section and oil stream simulations. Since the physical and mathematical models for the cross-sections are already given above, the physical and mathematical model for the oil stream are shown in Equations (8)–(10):

Mass conservation equation:

$$\frac{\partial}{\partial t}(\rho_o A)+\frac{\partial}{\partial z}(\rho_o v A)=0 \tag{8}$$

Energy conservation equation:

$$C_{p,o}\left(\frac{\partial\theta}{\partial t}+v\frac{\partial\theta}{\partial z}\right)-\frac{fv^3}{2d}=-\frac{4q}{\rho_o d} \tag{9}$$

Matching condition:

$$q = \lambda_1 \frac{\alpha T_\xi - \beta T_\eta}{J\sqrt{\alpha}} = h_o(T_w - \theta) \tag{10}$$

Among Equations (8), (9), and (10), θ denotes the hot oil temperature, v denotes the flow velocity of the oil stream, q denotes the heat flux between the oil stream and wax layer around the oil stream, and T_w stands for the temperature of the interface between the wax layer and oil flow, and its values are calculated by solving Equation (2). h_o represents the forced convection heat transfer coefficient of the oil flow and wax layer, which is a function of the oil temperature and must be determined by experimental data [22].

To solve Equations (7) and (8) under the matching conditions of Equation (9), the characteristics method is applied under the grid shown in Figure 10. Normally, the grid size along the pipe is between 0.5 km and 2 km.

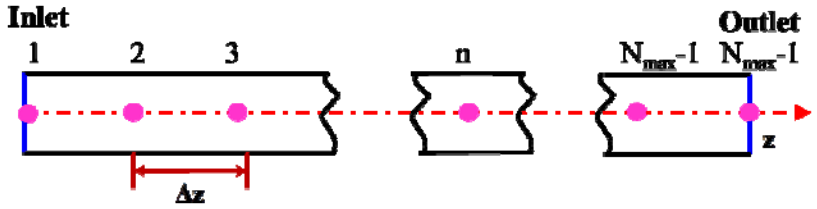

Figure 10. The grid along the pipe.

The final discretization of Equations (8) and (9) is shown in Equation (11):

$$\theta_i^n = \frac{\frac{f^{n-1}\left(v_i^{n-1}\right)^3}{2d_i} - \frac{4q_{i-1}^{n-1}}{\rho d_i} - C_{p,o}\frac{\theta_i^{n-1}-\theta_{i-1}^{n-1}}{\Delta z}v_i^{n-1} + \frac{C_{p,o}\theta_i^{n-1}}{\Delta t}}{C_{p,o}/\Delta t} \tag{11}$$

Equation (11) shows the superscript, n, means the present value and $n-1$ stands for the value in the previous time step. q_{i-1}^{n-1} in Equation (11) is the key variable, which binds the pipeline cross-sections' thermal simulation with the oil temperature calculation along the pipe. Using Equation (10), the value of q_{i-1}^{n-1} can be calculated after the temperature field in the cross-section is obtained by solving Equation (2).

4. Model Reduction for Pipeline's Cross-section Thermal Simulation

To realize the thermal simulation of the crude oil pipeline, Equation (2) and Equations (8)–(9) must be solved. During the thermal simulation of the crude pipeline, the most time-consuming part is its cross-sections' temperature field calculation (solving of Equation (2)), which can occupy more than 99.99% of the whole process. The authors of this paper try to adopt the POD reduced-order model to significantly improve the calculation speed.

Using the POD reduced-order model [19], the temperature can be written as Equation (12):

$$T(\xi, \eta, t) = \sum_{k=1}^{M} a_k(t)\phi_k(\xi, \eta) \tag{12}$$

where, $\phi_k(\xi, \eta)$ $(k = 1, 2, \ldots M)$ are the POD basis functions which are dependent on space (ξ, η) and independent of time, t. The basis functions can be obtained by analyzing the sampling data by POD. $a_k(t)$ $(k = 1, 2, \ldots M)$ are the amplitudes, which are dependent on time and independent of space. $a_k(t)$ $(k = 1, 2, \ldots M)$ are the unknowns and their equations are called the "reduced-order model". M is the order of basis functions to describe the temperature field and the dimensions of the unknowns, $a_k(t)$.

Equation (12) shows there are two key points in the POD reduced-order model, the POD basis functions and the reduced-order model. The POD basis function and reduced-order models

are introduced in Sections 4.1 and 4.2, respectively. The standard POD reduced-order model implementation procedure is introduced briefly in Section 4.3.

4.1. POD Basis Function

POD is a powerful mathematical method. Using the analysis on a set of simulation data (sampling matrix) obtained by full-order simulations, POD can extract a series of basis functions, which capture the dominant information of the physical problems. Regarding the unsteady-state heat transfer problem in this paper, the main process is as follows:

Suppose a two-dimensional unsteady-state heat transfer problem (such as the problem in this paper) of some specific conditions, which has N_ξ control points in the ξ direction and N_η control points in the η direction. The sampling matrix of this physical problem would be constructed.

The POD reduced-order model is applied to solve the unsteady problem with different conditions (boundary conditions and geometric shapes of the simulated domain) in this paper. The temperature fields at representative instances under various sampling conditions should be put into the sampling matrix. Suppose L kinds of sampling conditions are sampled and, for every condition, the temperature field at each time instance is obtained with a total number, K. Considering the ith condition, if the temperature fields in each time instance are sampled, the sampling matrix for the ith condition can be constructed as Equation (13). Similarly, for each condition, a sampling matrix for it can be obtained.

$$\mathbf{T}_i = \begin{bmatrix} T(\xi_1,\eta_1,t_1) & T(\xi_1,\eta_1,t_2) & \cdots & T(\xi_1,\eta_1,t_{K-1}) & T(\xi_1,\eta_1,t_K) \\ \vdots & \vdots & \cdots & \vdots & \vdots \\ T\left(\xi_{N_\xi},\eta_1,t_1\right) & T\left(\xi_{N_\xi},\eta_1,t_2\right) & \cdots & T\left(\xi_{N_\xi},\eta_1,t_{K-1}\right) & T\left(\xi_{N_\xi},\eta_1,t_K\right) \\ T(\xi_1,\eta_2,t_1) & T(\xi_1,\eta_2,t_2) & \cdots & T(\xi_1,\eta_2,t_{K-1}) & T(\xi_1,\eta_2,t_K) \\ \vdots & \vdots & \cdots & \vdots & \vdots \\ T\left(\xi_{N_\xi},\eta_2,t_1\right) & T\left(\xi_{N_\xi},\eta_2,t_2\right) & \cdots & T\left(\xi_{N_\xi},\eta_2,t_{K-1}\right) & T\left(\xi_{N_\xi},\eta_2,t_K\right) \\ \vdots & \vdots & \cdots & \vdots & \vdots \\ \vdots & \vdots & \cdots & \vdots & \vdots \\ T\left(\xi_1,\eta_{N_\eta},t_1\right) & T\left(\xi_1,\eta_{N_\eta},t_2\right) & \cdots & T\left(\xi_1,\eta_{N_\eta},t_{K-1}\right) & T(\xi_1,\eta_1,t_K) \\ \vdots & \vdots & \cdots & \vdots & \vdots \\ T\left(\xi_{N_\xi},\eta_{N_\eta},t_1\right) & T\left(\xi_{N_\xi},\eta_{N_\eta},t_2\right) & \cdots & T\left(\xi_{N_\xi},\eta_{N_\eta},t_{K-1}\right) & T\left(\xi_{N_\xi},\eta_1,t_K\right) \end{bmatrix} \quad (13)$$

What needs to be noted is the temperature of all the moments is not necessarily put into the sampling matrix, if the dominant information has been contained in the sampling matrix. Subsequent to a sampling matrix for each condition being obtained, all the matrices are combined to produce a larger sampling matrix, $\mathbf{S} \in \mathbb{R}^{m\times n}$, shown in Equation (14), where $m = N_\xi \times N_\eta$ and $n = \sum_{i=1}^{L} K_i$ (K_i is column number of $\mathbf{T}_i$). Thus, the matrix, $\mathbf{S}$, contains the information of the temperature evolution at time-bearing different conditions.

$$\mathbf{S}=\begin{bmatrix} \mathbf{T}_1 & \mathbf{T}_2 & \cdots & \mathbf{T}_L \end{bmatrix} \quad (14)$$

Using the "snapshot method" or "singular value decomposition (SVD) method" [9], the basis functions matrix can be obtained. Usually, to save the time consumption, the SVD method is adopted as $m < n$ and the "snapshot method" is used as $m > n$. Both methods are proper for $m = n$. In this paper, the SVD method is applied in Section 5.2. Thus, the SVD method is introduced as follows:

Consider the sampling matrix, $\mathbf{S} \in \mathbb{R}^{m\times n}$, with rank, $d \le min(m,n)$. Normally, in most engineering problems, there are no two same samplings put into a matrix, $\mathbf{S}$, $d = min(m,n)$. Since

the SVD method is only used as $m \leq n$, d is equal to m. The SVD method guarantees real numbers, $\sigma_1 \geq \sigma_2 \geq \ldots \geq \sigma_d > 0$, orthogonal matrices, $\mathbf{U} \in \mathbb{R}^{m \times m}$ and $\mathbf{V} \in \mathbb{R}^{n \times n}$, which satisfy Equation (15):

$$\mathbf{U^T S V} = \begin{pmatrix} \mathbf{D} & \mathbf{0} \\ \mathbf{0} & \mathbf{0} \end{pmatrix} \tag{15}$$

where, $\mathbf{D} = diag(\sigma_1, \ldots, \sigma_d) \in \mathbb{R}^{d \times d}$,U, and $\mathbf{V}$ are eigenvectors of $\mathbf{SS^T}$ and $\mathbf{S^T S}$, respectively. $\mathbf{U}$ and $\mathbf{V}$ are also called left singular vectors and right singular vectors. The first d columns of $\mathbf{U}$ and $\mathbf{V}$ are eigenvectors with eigenvalues, $\lambda_i = \sigma_i^2$, and the other columns are eigenvectors with eigenvalues, $\lambda_i = 0$. The first d columns in $\mathbf{U}$ are the POD basis functions required in the POD reduced-order model. Thus, the basis functions matrix, $\boldsymbol{\psi}$, can be written as Equation (16):

$$\boldsymbol{\psi} = \begin{bmatrix} \boldsymbol{\Phi}_1 & \boldsymbol{\Phi}_2 & \cdots & \boldsymbol{\Phi}_\mathrm{d} \end{bmatrix} \tag{16}$$

where, $\boldsymbol{\Phi}_k$ is the kth columns of $\mathbf{U}$, and $\boldsymbol{\Phi}_k$ can be expressed as Equation (17):

$$\boldsymbol{\Phi}_k = \left[\phi_k(\xi_1, \eta_1), \ldots, \phi_k(\xi_{N_\xi}, \eta_1), \phi_k(\xi_1, \eta_2), \ldots, \phi_k(\xi_{N_\xi}, \eta_2), \ldots, \ldots, \phi_k(\xi_{N_\xi}, \eta_{N_\eta})\right]^{\mathbf{T}} \tag{17}$$

4.2. Reduced-order model (equations of $a_k(t)$)

The reduced order model is established by projecting the governing equation, Equation (2), onto the space spanned by the first M basis functions. Following a series of deductions, the current research group established the BFC-based POD-Galerkin reduced-order model for the heat conduction problem (find the details in Ref. [20]), shown in Equation (18):

$$\sum_{k=1}^{M} \frac{\mathrm{d}a_k}{\mathrm{d}t} G_{ik} = -\left(\oint \sqrt{\alpha} q^{(\xi)} \phi_i d\eta - \sqrt{\gamma} q^{(\eta)} \phi_i d\xi \right) - \sum_{k=1}^{M} a_k H_{ik} i = 1, 2 \ldots M \tag{18}$$

where,

$G_{ik} = \int_\Omega J \rho c_p \phi_k \phi_i d\Omega.$

$H_{ik} = \int_\Omega \left[\frac{\lambda}{J} \left(\alpha \frac{\partial \phi_k}{\partial \xi} - \beta \frac{\partial \phi_k}{\partial \eta} \right) \frac{\partial \phi_i}{\partial \xi} + \frac{\lambda}{J} \left(\gamma \frac{\partial \phi_k}{\partial \eta} - \beta \frac{\partial \phi_k}{\partial \xi} \right) \frac{\partial \phi_i}{\partial \eta} \right] d\Omega$

Where the domain, Ω, here stands for the calculation domain on BFC shown in Figure 9. Equation (17) is a system of linear equations with $a_k (k = 1, 2, \ldots M)$ as unknowns, which can be solved by LU decomposition. Usually, for heat conduction problems, the value of M is below 30, which means the number of unknowns is below 30, while, in a full-order model, the unknowns can be thousands (3761 in the problem of this paper) or more, depending on the number of grids. Thus, the reduced-order model can reduce the order from thousands to less than 30, which makes the simulation speed increase significantly.

The boundary conditions are the same with the full-order model given above. The discretization of them in the POD reduced-order model can be found in Ref. [19].

4.3. The standard POD reduced-order model implementation procedure

Figure 11 gives the standard implementing procedure of the POD reduced-order model, which includes sampling, basis function extraction, reduced-order model solving, and physical field reconstructing. The details can be found in Reference [19].

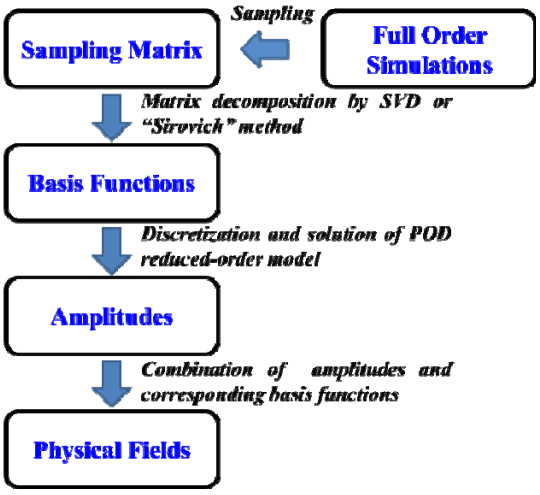

Figure 11. Procedure of proper orthogonal decomposition (POD) reduced-order model implementation.

5. Application and Discussions

The process of BFC-POD-ROM-aided fast thermal scheme determination for the Secondary Dong-Lin crude pipeline is elaborately introduced. First, the property and boundary variables of the pipeline are given. Subsequently, the implementation process and performance of the POD reduced-order model are illustrated. Finally, the thermal scheme for the Secondary Dong-Lin crude pipeline is determined and the results of the POD reduced-order model are compared with the field data.

5.1. Property and Boundary Variables for Secondary Dong-Lin crude Pipeline

To simulate the thermal behavior of the Secondary Dong-Lin pipeline, aside from the parameters given in Section 2, the property and boundary parameters should be given as well.

(1) Property parameters

Figure 8 shows there are several different-property domains in the physical mode of the pipeline, which are the oil stream, three layers, and soil region. Since the properties of the oils have been given in Section 2, only the property parameters of the soil and the three layers are offered here (see Table 2.).

Table 2. Properties of the soil and the three layers.

Soil and the three layers	ρ_i (kg/m^3)	$C_{p,i}$ (J/kg·°C)	λ_i (W/m·°C)
Soil (0 km–56 km)	2235	1.67	943
Soil (56 km–157.4 km)	2235	1.35	943
Anticorrosive Layer	1000	0.4	1670
Pipe-wall Layer	7850	50	460
Wax Layer	1000	0.15	2000

As shown in Table 2, the soil thermal conductivity from 0 km to 55 km of the pipeline is 1.67 W/m·°C, while the soil thermal conductivity becomes 1.35 W/m·°C after 56km of the pipeline. The heat conductivities are obtained by inverse calculation through the operational data of the Sinopec Company, which is a frequently-used method in oil pipeline thermal simulations [7].

(2) Boundary parameters

As shown in Figure 8, the boundary parameters of the pipeline cross-section include the temperature of the oil stream, θ, and the corresponding convective heat transfer coefficient, h_o, the

temperature of air, T_a, the corresponding convective heat transfer coefficient, h_a, and the temperature of the thermostat layer, T_{tl}.

θ can be determined through the match condition between the pipeline cross-section and oil stream, as shown in Equation (10), and h_o can be found by the empirical formula in Ref. [22] using the above boundary parameters. T_a is not the real temperature of air, rather a pseudo air temperature interpolated by the temperature of the thermostat layer (T_{tl}) and the measured value of soil temperature, T_b, in the buried depth of the crude oil pipeline, which has been a typical method in engineering for easy simulation [22]. The interpolation equation is shown in Equation (19):

$$T_a = T_b + \frac{T_b - T_{tl}}{H} H_b \tag{19}$$

where, H is the depth of the thermostat layer, and H_b is the buried depth of the oil pipe (See Figure 8).

Thus, the thermostat layer temperature, T_{tl}, soil temperature in a buried depth, T_b, and convective heat transfer coefficient, h_a, are the boundary parameters needed (see Table 3). Using field measurements for this study, T_{tl} is 12.3 °C and h_a is 20 (W/m^2·°C). T_b varies from day to day and mile to mile. Table 3 gives a series of field data in five typical spots measured by the Sinopec Company. T_b for other days and other spots are interpolated by the data from Table 3.

Table 3. Boundary parameters.

Soil Temperature in Buried Depth T_b (°C)					
Date	**0 km**	**30 km**	**55 km**	**106 km**	**157.4 km**
Oct. 31st 2015	22.67	22.44	20.28	20.75	24.76
Nov. 30th 2015	15.90	19.39	14.89	17.31	21.09
Dec. 31st 2015	7.39	13.39	9.94	12.71	15.68
Jan. 31st 2016	5.86	11.27	8.03	9.33	13.02
Feb. 29th 2016	5.23	10.14	7.24	8.32	11.31

5.2. POD-ROM-based fast thermal simulation for Secondary Dong-Lin crude pipeline

Figure 11 shows that to obtain the POD-ROM-based fast thermal simulation, there are two main steps. The first is sampling and basis function extracting. The second is reduced-order model solving and physical field reconstructing.

5.2.1. Sampling and Basis function

The quality of basis functions has a significant influence on the accuracy of POD reduced-order model-based fast thermal simulation. The acceptable basis functions should contain the main characters of the temperature field evolution of the Secondary Dong-Lin crude pipeline. This mainly depends on the sampling process, in which the samplings should be representative and, for sake of time consumption, as few as possible.

Figure 7 shows the whole pipeline is separated into a series of slices and the main differences among the slices are geometrics (see Figure 2) and boundary conditions (see Table 3). Thus, for this particular problem, the obtained temperature basis function must be capable of depicting the temperature field under different combinations of geometrics and boundary conditions. The main process for sampling and basis function extraction is as follows:

First, the sampling conditions are given in Tables 4–6. The sampling conditions are a thermal analogy of the real conditions. Take "Sampling 1" as an example: Sampling 1 is set as an analog of the thermal situation of the 0–20 km part in the Secondary Dong-Lin crude pipeline. To obtain such an analog, the geometry and heat conductivity of Sampling 1 are set the same within the 0–20km part in the Secondary Dong-Lin crude pipeline. To save time in the samplings' calculation, the samplings' simulation times are set at 50 days, which is much shorter than the real conditions (five months). The alternate frequency (1.5 d/3.5 d one time) is also much higher than the real conditions. The real

T_b (soil temperature in buried depth) changes from month to month so are analogized by changing it every 10 days (see Table 6).

Table 4. The samplings.

Sampling No.	Geometry (See Table 5)	T_b (°C)	λ_4 (W/m·°C)	θ_h (°C)	θ_l (°C)	t_h/t_l (d/d)	T_{initial} (°C)	t_s (d)
1	Geo1	See Table 6	1.67	23	38	1.5/3.5	0	50
2	Geo2			20	38		45	
3	Geo3			15	35		75	
4	Geo4		1.35	14	36	0.5/1.5	105	
5	Geo5			13	35		157	

Note: T_{initial} (0) stands for the temperature field in the 0 km zone of the crude pipeline before the commission of the batching transportation scheme. T_{initial} (45) stands for the temperature field at 45 km. The others follow in kind.

Table 5. Geometry parameters of Geo1–Geo5.

Geo No.	d (m)	H_b (m)	δ_w (m)	δ_{ac} (m)
Geo 1	φ616 × 7	1.315	0.003	0.007
Geo2	φ616 × 7	1.915	0.003	0.007
Geo3	φ695 × 8	1.3555	0.003	0.007
Geo4	φ695 × 8	1.5555	0.003	0.007
Geo5	φ695 × 8	1.8555	0.003	0.007

Table 6. T_b at different times.

Time	0 d–10 d	10 d–20 d	20 d–30 d	30 d–40 d	40 d–50 d
T_b (°C)	22.67	15.9	7.39	5.86	5.23

Subsequently, using FVM, the temperature field in each slice is calculated with time steps at 600s on body-fitted grids (grid number is 3761), as shown in Figure 12.

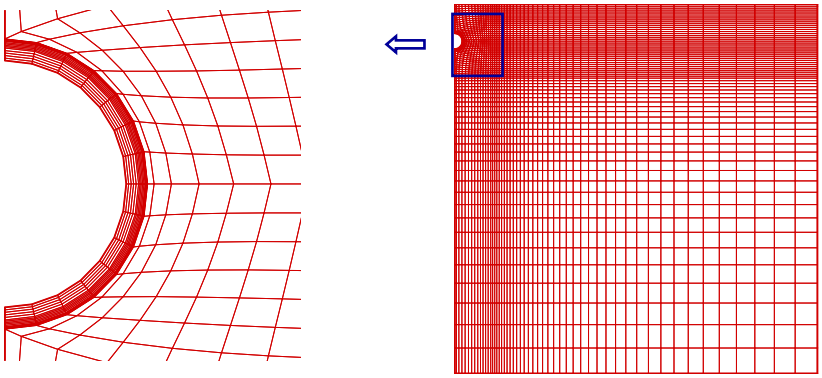

Figure 12. Body-fitted coordinate-based (BFC) grid of the pipeline cross-section.

Based on the temperature fields obtained by the FVM, the sampling matrix shown in Equation (14) can be constructed. To reduce the dimension of the sampling matrix (which can cause problems for the matrix decomposition) and avoid unnecessary information noise, sampling is dense when the temperature field changes quickly. Quite the reverse, it is sparse when the temperature field is changing slowly.

Thus, for this particular problem, the temperature field in every time step is put into the sampling matrix in time intervals [0 h, 5 h] after the alternates of θ_h and θ_l. One temperature field is adopted every five and 10 time steps in the time interval [5 h, 10 h] and [10 h, t_h or t_l], respectively. To summarize,

the sampling matrix, **S**, shown in Equation (14) consists of 8330 temperature fields, which makes **S** a matrix with 3761 rows and 8330 columns.

Finally, the basis functions are extracted from the sampling matrix, **S**, by SVD. The energy distribution of basis functions is shown in Figure 13. The first 23 basis functions, $M = 23$ in Equation (12), are applied into the POD reduced-order model for fast simulation. Figure 14 gives contours of four typical basis functions based on Geo 1.

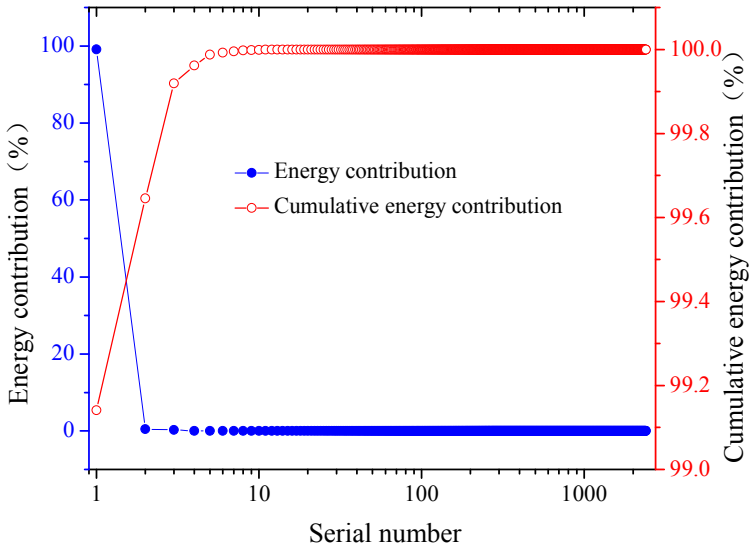

Figure 13. Energy distribution of basis functions.

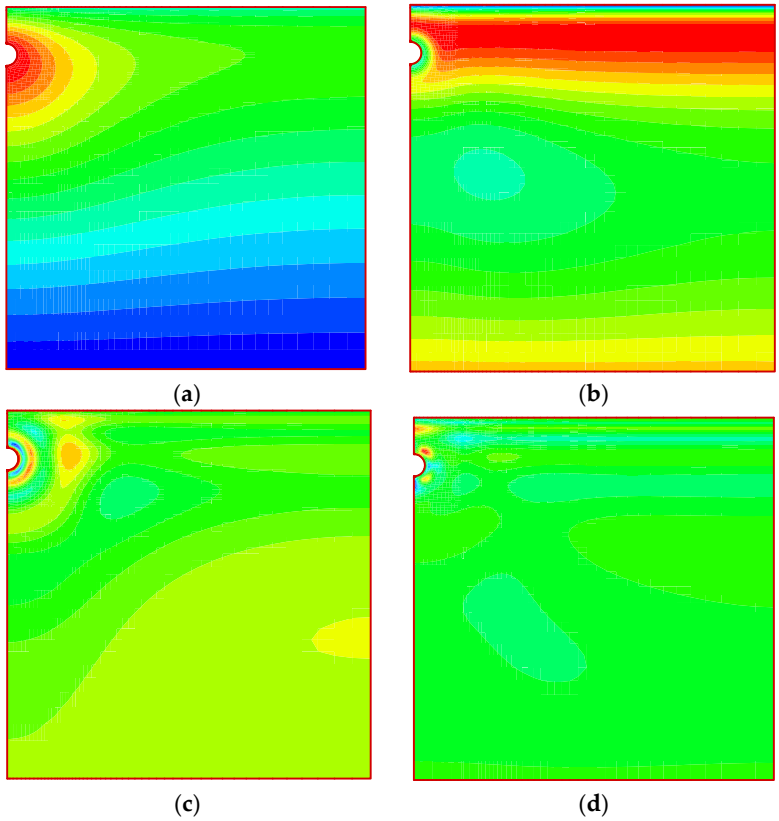

Figure 14. Contours of four typical basis functions based on Geo 1: (**a**) 1st; (**b**) 5th; (**c**) 15th; (**d**) 23rd.

5.2.2. POD Reduced-order model validation and thermal characteristics of batch transportation

To test the accuracy of the POD reduced-order model-based fast simulation, the first three potential schemes (see Table 7) given by Sinopec are simulated by a POD reduced-order model as well as the FVM.

Table 7. Parameters for Schemes 1–3.

Scheme No.	Q_h^D/Q_l^D (m^3h^{-1}/m^3h^{-1})	Q_h^{BI} (m^3h^{-1})	θ_h/θ_l (°C/°C)	t_h/t_l (d/d)	r_{SL}/r_{OM}
1	2161/2470	172	See Table 8	7.56/2.44	90:36
2	2322/2321			8.11/2.83	90:26
3	1872/2470			7.56/2.44	90:20

Table 8. Values of θ_h and θ_l in different months.

Time	θ_l (°C)	θ_h (°C)			Furnaces
		Scheme 1	Scheme 2	Scheme 3	
Oct. 2015	23.20	37.03	38.22	39.04	Both furnaces in Dongying and Binzhou are closed
Nov. 2015	20.00	36.37	37.78	38.75	
Dec. 2015	14.88	33.77	35.39	36.51	
Jan. 2016	13.60	33.89	35.64	36.84	
Feb. 2016	12.90	33.69	35.48	36.71	

Regarding the Secondary Dong-Lin crude pipeline, the coldest month each year is February. The environmental temperature decreased progressively from October 2015 to February 2016, as shown in Table 3, which made February 2016 the riskiest month. The oil temperature distribution has great significance for engineering. Considering Scheme 1, the oil temperature distributions during the last cycle (the last 2.44 d/7.56 d) in February 2016 are shown in Figure 15.

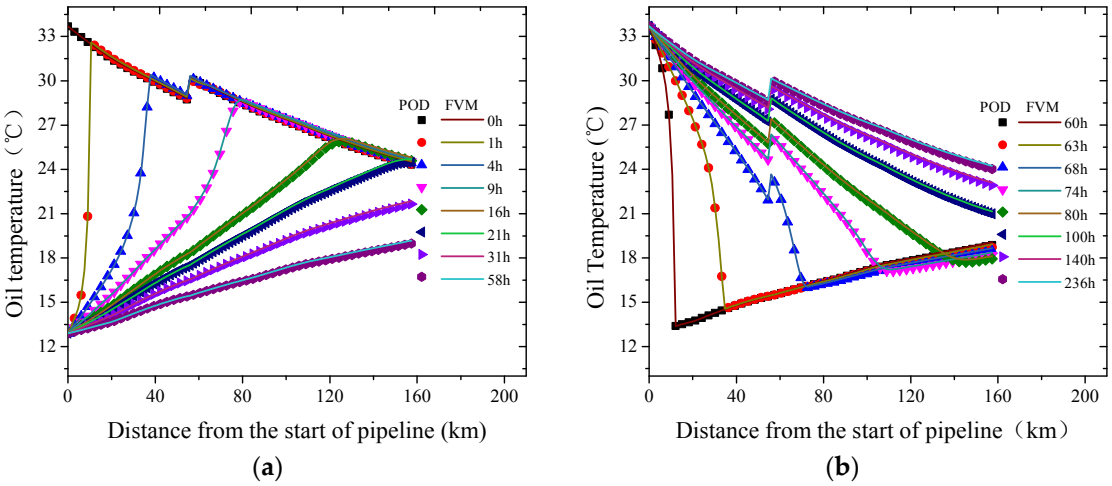

Figure 15. The oil temperature along the pipeline during the last cycle of Scheme 1: (**a**) 0 d–2.44 d; (**b**) 2.44 d–10 d.

The curves in Figure 15 are explained as follows: Beginning with the last cycle, t = 0 h in Figure 15a, the whole pipeline is filled with SL_{OM} oil. Table 8 shows the temperature of the oil in z = 0 km is 33.69 °C and, due to the heat loss to the environment, the temperature decreases along the pipeline from 0 km to 55 km. Since the injected SL_{OM} oil in z = 55 km is at 50 °C (higher than the upstream SL oil's temperature of 28.73 °C), the mixed oil becomes 30.18 °C, which shows a temperature jump at z = 55 km (See Figure 15a). The temperature after z = 55 km decreases for the earlier stated reason before z = 55 km.

Then, the OM oil, at 12.9 °C, is pumped into the pipeline, which is at a lower temperature than the SL oil's temperature. Thus, the OM oil is warmed when it flows along the pipeline, which can be shown by the curves at t = 1 h, 4 h, and 9 h. What should be noted is that the oil pipeline is not occupied fully by the OM oil until t = 16 h. Thus, the curves of t = 1 h, 4 h, and 9h show an up-and-down trend. The "uptrend-curves" part of the pipeline is filled with OM oil, which absorbs energy from the environment. The "downtrend-curves" part of the pipeline is filled with SL_{OM} oil, which releases energy to the environment. When at t = 16 h, the SL oil is completely driven out of the pipeline by the OM oil behind.

While the OM oil keeps absorbing the energy from the environment, the temperature of the environment decreases, leading to the OM oil temperature decreasing with time, as shown in Figure 15a. The "reduction" lasts until the oils alternate at the beginning of the pipeline. Figure 15b shows the temperature curves after the alternation. It illustrates the opposite thermal characteristics of Figure 15a, when SL_{OM} oil with a higher temperature than OM oil is pumped into and fully occupies the pipeline.

Figure 15a,b have the symbols and lines representing the results of the POD reduced-order model and the FVM, respectively. Even though the thermal characteristics of the Dong-Lin crude pipeline are very complicated, as stated above, the results of the POD reduced-order model agree well with those of the FVM. The main thermal characteristics along the pipeline of Schemes 2 and 3 are similar to those of Scheme 1, given in Figure 15, and the differences are just the values. Aside from the oil temperature distribution along the pipeline, the engineers are also concerned about the oil temperature flowing out of the pipeline. Thus, for the three schemes, Figure 16 gives the outflow oil temperature (in the end of the pipeline) versus time curves.

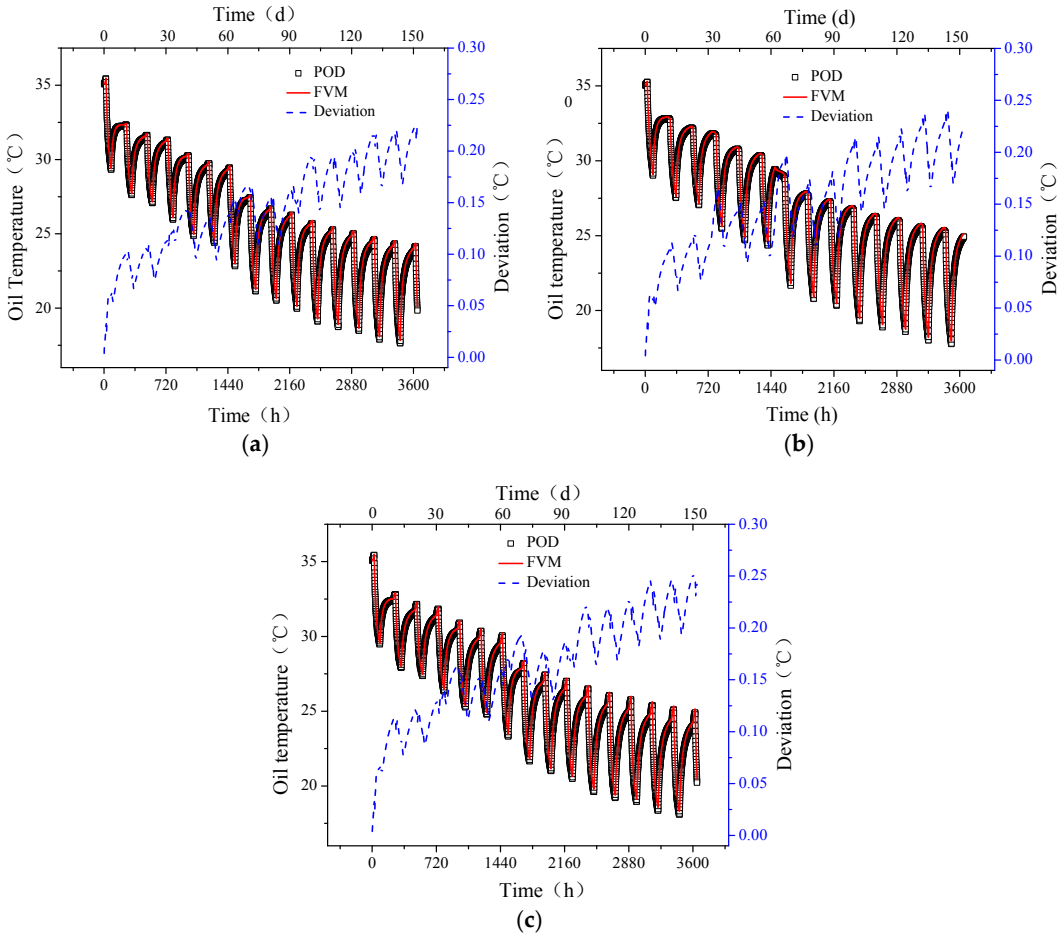

Figure 16. The oil temperature flowing out of the pipeline in Linyi Station: (**a**) Scheme 1; (**b**) Scheme 2; and (**c**) Scheme 3.

Figure 16 shows the oil temperature in the end of the pipeline periodically declines from October 2015 to February 2016. The periodic alternating of the oils pumped into the pipeline and the increasingly colder weather are responsible for the two trends. Looking at Figure 16, it can be found that the POD reduced-order model has good accuracy. The largest errors (compared with the FVM) for Schemes 1, 2, and 3 are 0.22 °C, 0.24 °C, and 0.25 °C, respectively. The mean errors (compared with FVM) for Schemes 1, 2, and 3 are 0.15 °C, 0.15 °C, and 0.16 °C, respectively.

To illustrate the accuracy of the POD reduced-order model more vividly, for Scheme 1, Figures 17 and 18, respectively, give the temperature fields at the beginning and end of the pipeline. Figures 17 and 18 have dashed lines representing the POD reduced-order model results and solid lines representing the FVM. The results agree well with each other.

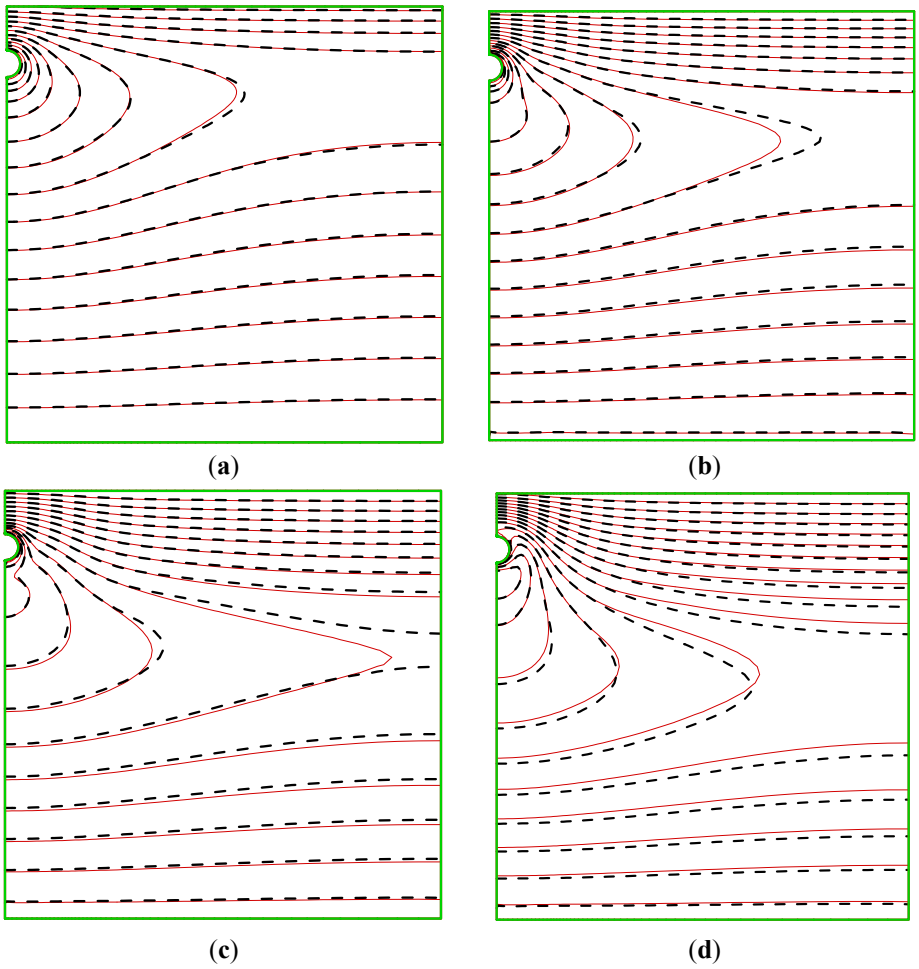

Figure 17. The cross-section's temperature field in the beginning of the pipeline (dashed lines: POD reduced-order model. Solid lines: Finite volume method (FVM)): (**a**) 38th day; (**b**) 76th day; (**c**) 114th day; (**d**) 152nd day.

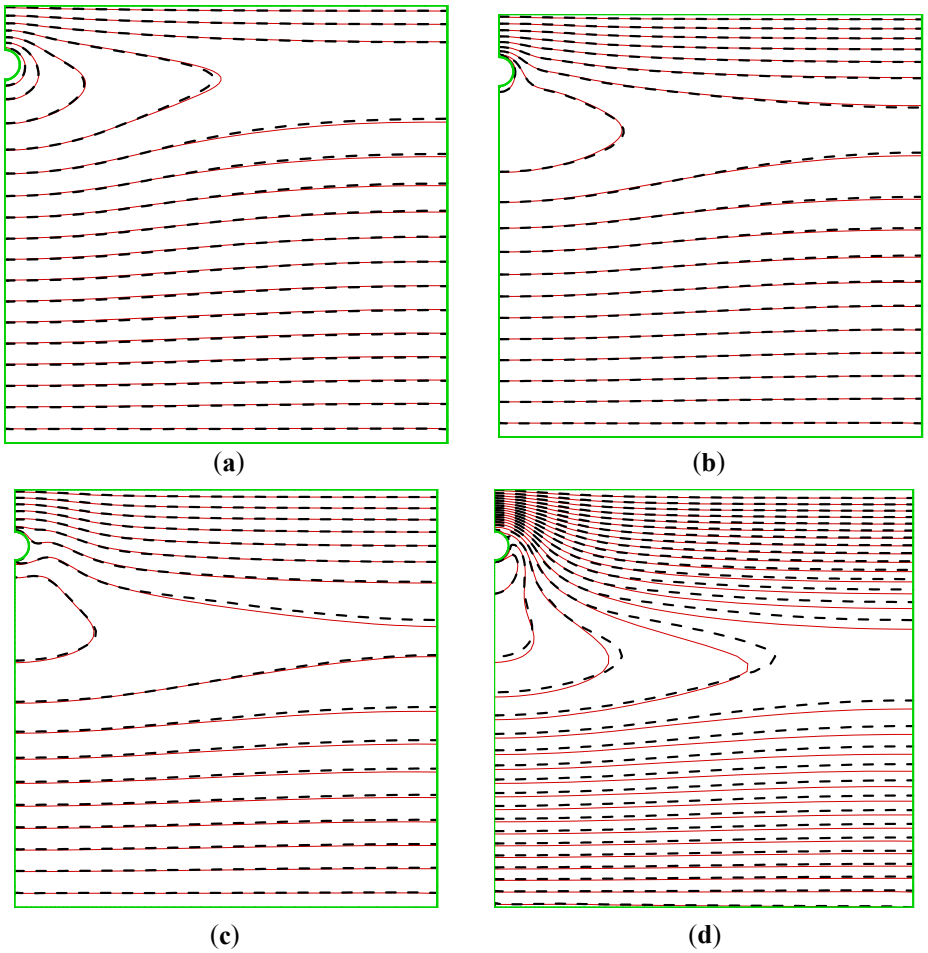

Figure 18. The cross-section's temperature field at the end of the pipeline (Dashed lines: POD reduced-order model. Solid lines: FVM): (**a**) 38th day; (**b**) 76th day; (**c**) 114th day; (**d**) 152nd day.

To illustrate the speed advantage of the POD reduced-order model, Table 9 shows the time consumption of the POD reduced-order model and the FVM. The simulation speed is more than 100 times faster than the FVM, which means much time is saved in the engineering.

Table 9. Time consumptions of the FVM and POD reduced-order models.

Scheme No.	FVM (h)	POD (h)	Acceleration Factor
Scheme 1	62.7	0.49	128
Scheme 2	64.5	0.52	124
Scheme 3	64.0	0.56	114

Considering the above analysis, it can be found that, for the thermal simulation of the Dong-Lin crude pipeline with oil batching transportation, the POD reduced-order model has good accuracy and significant efficiency. Thus, rather than the commonly-used FVM, the POD reduced-order model is adopted to determine the operational scheme in this paper.

5.3. Detail Batch Transportation Scheme Determination and Field Verification

Through the first three potential schemes given by Sinopec, the performance of the POD reduced-order model was verified. Following that, considering the capacity of oil stocks, blend ratios of SL_{OM} oils, behaviors of furnaces, and other factors, the Sinopec Company drew 1024 potential schemes in sum. All the schemes were simulated by the POD reduced-order model to find their

thermal performance critical to the energy cost of the oil heated and oil pumped because oil fluidity is related to oil temperature (see Figure 4).

Considering the thermal and hydraulic consumption of each scheme given by the simulations, the Sinopec Company chose Scheme No. 124 (shown in Table 10) as the final operating scheme based on the considerations of power consumption and transportation risk. The risk means the restart-ability of the oil pipeline after being shut-down for an accident. The lower the temperature and the longer the shut-down time, the higher the risk is.

Table 10. Parameters for the determined scheme.

Scheme No.	Q_h^D/Q_l^D (m^3h^{-1}/m^3h^{-1})	Q_h^{BI} (m^3h^{-1})	θ_h/θ_l (°C/°C)	t_h/t_l (d/d)	r_{SL}/r_{OM}
124	1370/2064	172	See Table 11	4.58/1.17	9:2

Table 11. The determined values of θ_h and θ_l in different months.

Time	θ_l (°C)	θ_h (°C)	Furnace in Dongying	Furnace in Linyi
Oct. 2015	23.5	41.5	Close for OM oil. Open for SL_{OM} oil and keep heating it to 41.5 °C	Open for both OM and SL_{OM} oil Raise OM oil 8 °C Raise SL_{OM} oil 5 °C
Nov. 2015	23	41.5		
Dec. 2015	21	41.5		
Jan. 2016	19	41.5		
Feb. 2016	17	41.5		

To ensure the success of the new scheme commissioning, the Sinopec Company did much more preparation than was expected. Thus, the company began to execute the chosen scheme on November 4, 2015. Figure 19 gives the comparisons between the simulated results and the operational field data.

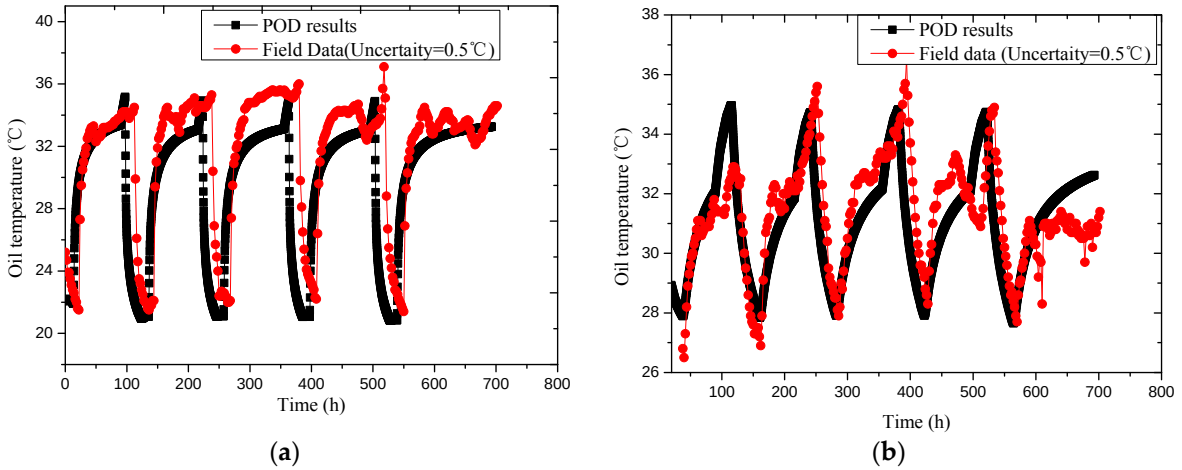

Figure 19. The comparisons between field data and the results predicted by the POD reduced-order model: (**a**) The oil temperature flowing into Binzhou station versus time on February 2016; (**b**) the oil temperature flowing into Linyi station versus time on February 2016.

Figure 19 demonstrates the thermal behavior under the chosen scheme can be predicted with an error acceptable to crude oil engineering. There are some spikes in the field data shown in Figure 19. The flow flux and the temperature are not controlled precisely during real-time engineering, which means the pipeline is operated around the chosen scheme, and not exactly on the scheme. To operate a crude oil pipeline exactly according to the planning scheme is impossible due to unpredictable factors (such as the flow shock of the upstream, and the temporary change of oil transportation task) existing in practical engineering.

The oil temperature flowing into other stations shows the same behavior. To properly describe the deviations between the field data and simulation results, the mean oil temperatures flowing into Binzhou and Linyi station are calculated. It should be noted that the mean temperature of OM oil and SL_{OM} oil are calculated independently (see Tables 12 and 13). The deviations are also shown in Tables 12 and 13.

Table 12. The mean temperature of OM oil in different months.

Oil	Data	Nov. 2015		Dec. 2015		Jan. 2016		Feb. 2016	
θ_{OM} in BZ	Field Data	28.89	(0.24, 0.8%)	26.78	(0.48, 1.8%)	25.66	(1.21, 4.7%)	23.54	(0.42, 1.8%)
	POD Results	29.13		26.30		24.45		23.12	
θ_{OM} in LY	Field Data	32.18	(1.27, 3.9%)	32.93	(0.15, 0.4%)	29.62	(0.48, 1.6%)	29.98	(0.32, 1.1%)
	POD Results	33.45		33.08		30.10		30.30	

Note: BZ is for Binzhou station and LY is for Linyi station. The values in the brackets are absolute and relative deviations, respectively.

Table 13. The mean temperature of SL_{OM} oil in different months.

Oil	Data	Nov. 2015		Dec. 2015		Jan. 2016		Feb. 2016	
$\theta_{SL_{OM}}$ in BZ	Field Data	36.02	(0.12, 0.3%)	35.66	(0.48, 1.3%)	33.89	(1.21, 3.6%)	33.64	(0.06, 0.2%)
	POD Results	36.14		36.35		34.63		33.58	
$\theta_{SL_{OM}}$ in LY	Field Data	33.99	(0.99, 2.9%)	34.48	(1.37, 4.0%)	31.29	(0.79, 2.5%)	31.72	(0.63, 2.0%)
	POD Results	34.98		35.85		32.08		32.35	

Note: BZ is for Binzhou station and LY is for Linyi station. The values in the brackets are absolute and relative deviations, respectively.

Tables 12 and 13 show the mean oil temperature errors are less than 1.27 °C and 1.37 °C for OM and SL_{OM} oil, respectively, which is acceptable for oil transportation engineering. There are three reasons to generate such a deviation. First, the physical model used in the current study is an approximate description and the POD reduced-order model itself is also an approximate mathematical model. Second, there are some inevitable errors in parameter values in the physical model, such as the heat capacity, density and viscosity of oil, the heat conductivity in the regions of the wax layer, pipe-wall layer, anticorrosive layer, and soil, and the forced convection heat transfer coefficient of the oil flow and the wax layer. Third, the pipeline is operated around the chosen scheme, not exactly on the scheme, as stated above, which is believed to be the biggest reason.

To summarize, the BFC-based POD-ROM is adopted to determine the detailed scheme to improve the efficiency more than a hundred times. Compared with the FVM, the POD reduced-order model reduces the simulation time from 264 days, using 10 computers' parallel computing, to 2.2 days. The Dong-Lin crude oil pipeline has been safely operating for more than two years using the determined scheme.

6. Conclusions

The determination of the crude pipeline's detailed batch transportation scheme could cost tremendous thermal simulation time, which is an unsolved problem in oil transportation engineering. To solve this problem for China's Secondary Dong-Lin crude pipeline, a fast scheme determination strategy was developed for the first time.

The main idea of the strategy was that, rather than the traditional FVM, the BFC-based POD reduced-order model was adopted to increase the speed of the thermal simulation. The whole strategy included three main steps, which are summarized as follows:

(1) Sampling matrix construction and basis function obtainment.

The quality of basis functions has significant influence on the accuracy of the POD reduced-order model-based fast thermal simulation. Thus, the corresponding samplings should be representative and, for the sake of time consumption, as few as possible. Regarding crude oil batch transportation,

the following point is recommended: Design the sampling conditions by using the "analogy method", which means the geometry and heat conductivity should be the same within the pipeline and the boundary condition can be designed as an analogy of the real condition (see Tables 4–6). To reduce the dimensions of the sampling matrix, sampling can be dense as the temperature field changes quickly and sparse as the temperature field is slowly changing.

(2) The validation of the POD reduced-order model.

The POD reduced order model is an approximate method. Its accuracy is dependent on the quality of obtained basis functions, the number of basis functions adopted in the POD reduced-order model, and the complexity of the problem. Thus, the POD reduced-order model should be validated by the full order model (FVM in this paper) before being applied to the engineering.

Regarding the specific problem in this paper, through the comparisons between the POD reduced-order model and FVM, it was found that the POD reduced-order model had good accuracy with a mean error of 0.16 °C, which is acceptable for engineering. Thus, it is believed the POD reduced-order model can be applied to thermal simulations of crude oil batch transportation. The obtained basis function is feasible for China's Secondary Dong-Lin crude pipeline and the number of adopted basis functions is appropriate.

(3) The determination of the transportation scheme.

It was found that the POD reduced-order model can be more than one hundred times faster than the FVM. Therefore, to find a proper operational scheme, it is feasible to simulate hundreds, or thousands of schemes with reasonable time consumption. Moreover, this method can be combined with some optimization methods to find an optimized operating scheme.

Aided by the body-fitted coordinate-based POD reduced-order model, the details of the batch transportation scheme were determined and can be found in Tables 10 and 11. The Dong-Lin crude oil pipeline has been safely operating for more than two years using the determined scheme. Compared with the field data, the predicted results by the POD reduced-order model are of an acceptable accuracy for crude oil engineering. The mean oil temperature errors were less than 1.27 °C and 1.37 °C for OM and SL_{OM} oil, respectively.

Author Contributions: Conceptualization, B.Y.; Methodology, D.H.; Code, D.H.; Validation, Q.Y., D.C. and G.Z.; Writing—Original Draft Preparation, D.H.; Writing—Review & Editing, B.Y., D.H., and Q.Y.

Funding: The study is supported by National Science Foundation of China (No. 51706021), The Beijing Youth Talent Support Program (CIT&TCD201804037), the Jointly Projects of. Beijing Natural Science Foundation and Beijing Municipal Education Commission (KZ201810017023) and the Project of Construction of Innovative Teams and Teacher Career Development for Universities and Colleges Under Beijing Municipality (No. IDHT20170507).

Conflicts of Interest: The authors declare no conflict of interest.

Nomenclature

Roman Symbols

a_k	Amplitude of the kth POD basis function
A	Flowing area of the pipeline (m^2)
$c_{p,i}$	Specific heat capacity of region i (J/(kg·°C))
$c_{p,o}$	Specific heat capacity of oil (J/(kg·°C))
d	Diameter of the pipeline (mm)
f	The Darcy coefficient
h_o	Heat convection coefficient between the wax layer and oil stream ($W/(m^2 \cdot °C)$)
h_a	Heat convection coefficient between the soil and air ($W/(m^2 \cdot °C)$)
H	Thermal influence region on the vertical direction (m)
H_b	The buried depth of crude oil pipeline (m)
L	Thermal influence region on the horizontal direction (m)

q	The heat flux between the wax layer and oil stream (W/m^2)
Q_h^D, Q_l^D	Flow flux of hot and cool oil in Dongying station (m^3/h)
Q_h^{BI}	The flow flux injected in Binzhou station (m^3/h)
$r_{\mathrm{SL}}, r_{\mathrm{OM}}$	Ratio of SL oil and OM oil in $\mathrm{SL_{OM}}$ oil
$\mathbf{S}$	The sampling matrix
t_h	Transportation time of hot oil during one period (h)
t_l	Transportation time of cool oil during one period (h)
t_s	The total transportation time of hot and cool oils (h)
T	Temperature of the pipeline's cross-section
T_a	Temperature of the air (°C)
T_c	Temperature of the soil thermostat layer (°C)
v	Flow velocity of the oil stream (m/s)
x, y	Cartesian coordinate in the cross-section of pipeline (m)
z	Coordinate along the cross-section of pipeline (m)
Greek Symbols	
δ_w	Thickness of the wax layer (m)
δ_{ac}	Thickness of the anticorrosive layer (m)
ϕ_k	The kth POD basis function
$\mathbf{\Phi}_k$	Vector of the kth POD basis function
λ_i	Heat conductivity coefficient of region i (W/(m·°C))
μ	Viscosity (Pa·s)
θ	Temperature of the oil (°C)
θ_{cp}	Condensation point of crude oil (°C)
θ_h	Temperature of the hot oil, namely $\mathrm{SL_{OM}}$ oil (°C)
θ_l	Temperature of the cool oil, namely OM oil (°C)
$\theta_{\mathrm{SL_{OM}}}$	Temperature of $\mathrm{SL_{OM}}$ oil (°C)
θ_{OM}	Temperature of OM oil (°C)
ρ_i	Density of region i (W/(m·°C))
ρ_o	Density of oil (kg/m^3)
ξ, η	Body-fitted coordinate in the cross-section of pipeline (m)
Subscripts	
1,2,3,4	Regions of wax layer, pipe-wall layer, anticorrosive layer and soil respectively
ac	Anticorrosive layer
h	Hot oil
l	Cool oil, namely low temperature oil
o	oil
OM	Oman oil
SL	Shengli oil
$\mathrm{SL_{OM}}$	Mixture of SL oil and OM oil
tl	Thermostat layer
w	Wax layer
ξ, η	Partial derivatives of the variable

References

1. Yu, Y.; Wu, C.; Xing, X.; Zuo, L. Energy saving for a Chinese crude oil pipeline. In Proceedings of the ASME 2014 Pressure Vessels and Piping Conference, Garden Grove, CA, USA, 20–24 July 2014. [CrossRef]
2. Zhang, H.R.; Liang, Y.T.; Xia, Q.; Wu, M.; Shao, Q. Supply-based optimal scheduling of oil product pipelines. *Petrol. Sci.* **2016**, *13*, 355–367. [CrossRef]
3. Shauers, D.; Sarkissian, H.; Decker, B. California line beats odds, begins moving viscous crude oil. *Oil Gas J.* **2000**, *98*, 54–66.
4. Mecham, T.; Wikerson, B.; Templeton, B. Full Integration of SCADA, field control systems and high speed hydraulic models-application Pacific Pipeline System. In Proceedings of the International Pipeline Conference, Calgary, AB, Canada, 1–5 October 2000. [CrossRef]

5. Cui, X.G.; Zhang, J.J. The research of heat transfer problem in process of batch transportation of cool and hot oil. *Oil Gas Stor. Trans.* **2013**, *23*, 15–19. [CrossRef]
6. Wang, K.; Zhang, J.J.; Yu, B.; Zhou, J.; Qian, J.H.; Qiu, D.P. Numerical simulation on the thermal and hydraulic behaviors of batch pipelining crude oils with different inlet temperatures. *Oil Gas Sci. Technol.* **2009**, *64*, 503–520. [CrossRef]
7. Yuan, Q.; Wu, C.C.; Yu, B.; Han, D.; Zhang, X.; Cai, L.; Sun, D. Study on the thermal characteristics of crude oil batch pipelining with differential outlet temperature and inconstant flow rate. *J. Petrol. Sci. Eng.* **2018**, *160*, 519–530. [CrossRef]
8. Lumley, J.L. *The Structure of Inhomogeneous Turbulent Flows in Atmospheric Turbulence and Radio Wave Propagation*; Nauka: Moscow, Russian, 1967.
9. Sirovich, L. Turbulence and dynamics of coherent structures, Part 1: Coherent structures. *Q. Appl. Math.* **1987**, *45*, 561–571. [CrossRef]
10. Huang, N.E.; Shen, Z.; Long, S.R.; Wu, M.L.; Shih, H.H.; Zheng, Q.; Yen, N.C.; Tung, C.C.; Liu, H.H. The empirical mode decomposition and Hilbert spectrum for nonlinear and nonstationary time series analysis. *Proc. Roy. Soc. London A* **1998**, *454*, 903–995. [CrossRef]
11. Schmid, P.J. Dynamic mode decomposition of numerical and experimental data. *J. Fluid Mech.* **2010**, *656*, 5–28. [CrossRef]
12. Banerjee, S.; Cole, J.V.; Jensen, K.F. Nonlinear model reduction strategies for rapid thermal processing systems. *IEEE Trans. Semiconduct. Manuf.* **1988**, *11*, 266–275. [CrossRef]
13. Raghupathy, A.P.; Ghia, U. Boundary-condition-independent reduced-order modeling of complex 2D objects by POD-Galerkin methodology. In Proceedings of the IEEE Semiconductor Thermal Measurement and Management Symposium, San Jose, CA, USA, 15–19 March 2009. [CrossRef]
14. Fogleman, M.; Lumley, J.; Rempfer, D.; Haworth, D. Application of the proper orthogonal decomposition to datasets of internal combustion engine flows. *J. Turbul.* **2004**, *5*, 1–18. [CrossRef]
15. Ding, P.; Tao, W.Q. Reduced order model based algorithm for inverse convection heat transfer problem. *J. Xi'an Jiaotong Univ.* **2009**, *43*, 14–16. [CrossRef]
16. Thomas, A.B.; Raymond, L.F.; Pau, G.A.; Thomas, J.; Breault, R.W. A reduced-order model for heat transfer in multiphase flow and practical aspects of the proper orthogonal decomposition. *Theor. Comp. Fluid Dyn.* **2012**, *43*, 68–80. [CrossRef]
17. Gaonkar, A.K.; Kulkarni, S.S. Application of multilevel scheme and two level discretization for POD based model order reduction of nonlinear transient heat transfer problems. *Comput. Mech.* **2015**, *55*, 179–191. [CrossRef]
18. Selimefendigil, F.; Öztop, F. Numerical study of natural convection in a ferrofluid-filled corrugated cavity with internal heat generation. *Numer. Heat Tr. A-Appl.* **2015**, *67*, 1136–1161. [CrossRef]
19. Han, D.; Yu, B.; Yu, G.; Zhao, Y.; Zhang, W. Study on a BFC-based POD-Galerkin ROM for the steady-state heat transfer problem. *Int. J. Heat Mass Tran.* **2014**, *69*, 1–5. [CrossRef]
20. Han, D.; Yu, B.; Zhang, X. Study on a BFC-Based POD-Galerkin Reduced-Order Model for the unsteady-state variable-property heat transfer problem. *Numer. Heat Tr. B-Fund.* **2014**, *65*, 256–281. [CrossRef]
21. Yu, G.; Yang, Q.; Dai, B.; Fu, Z.; Lin, D. Numerical study on the characteristic of temperature drop of crude oil in a model oil tanker subjected to oscillating motion. *Energies* **2018**, *11*, 1229. [CrossRef]
22. Yang, Y.H. *Design and Management of Oil Pipeline*, 1st ed.; Press of China Petroleum University: Qing Dao, China, 2006.
23. Cheng, Q.; Gan, Y.; Su, W.; Liu, Y.; Sun, W.; Xu, Y. Research on exergy flow composition and exergy loss mechanisms for waxy crude oil pipeline transport processes. *Energies* **2017**, *10*, 1956. [CrossRef]
24. Tao, W.Q. *Numerical Heat Transfer*; Xi'an Jiaotong University Press: Xi'an, China, 2001.